CHARACTERIZATION OF ELECTRON-BEAM-EXPOSED NEGATIVE RESISTS

by

Nelson N. S. Tam

Memorandum No. UCB/ERL M88/32

20 May 1988

CHARACTERIZATION OF ELECTRON-BEAM-EXPOSED NEGATIVE RESISTS

by

Nelson N. S. Tam

Memorandum No. UCB/ERL M88/32

20 May 1988

ELECTRONICS RESEARCH LABORATORY

College of Engineering
University of California, Berkeley
94720

CHARACTERIZATION OF ELECTRON-BEAM-EXPOSED NEGATIVE RESISTS

by

Nelson N. S. Tam

Memorandum No. UCB/ERL M88/32

20 May 1988

ELECTRONICS RESEARCH LABORATORY

College of Engineering
University of California, Berkeley
94720

Nelson N. S. Tam

Author

Characterization of Electron-Beam-Exposed Negative Resists

Title

RESEARCH PROJECT

Submitted to the Department of Electrical Engineering and Computer Sciences, University of California, Berkeley, in partial satisfaction of the requirements for the degree of Master of Sciences, Plan II.

Approval for the Report and Comprehensive Examination:

Committee: Andrew R. Neureuther, Research Adviser

5/10/88 Date

W. G. Oldham, Second Reader

5/9/88, Date

Characterization of Electron-Beam-Exposed Negative Resists

Nelson Tam

Department of Electrical Engineering and Computer Science
and Electronics Research Laboratory
University of California
Berkeley, California 94720

ABSTRACT

The behavior of Hitachi RD-2000N and Shipley ECX-1033 negative resists under electron-beam exposure at high-beam current density on the AEBLE-150 has been characterized and modeled through dissolution measurement on the Perkin-Elmer Development Rate Monitor (DRM) and SAMPLE simulation. A quantitative model with three parameters relating dissolution-rate to deposited-energy has been established. Utilizing this model, SAMPLE can predict accurately resist thickness-remaining in relation to dose and simulate resist profile development. With the high-beam current density exposure available on the AEBLE-150, RD-2000N shows noticeable increase of resist thickness top loss at high dose region and rough resist surface topography at 25A/cm^2. This change in development behavior is consistent with thermal heating of the top of the resist during exposure. Initial data on the AEBLE-150 showed lower contrast (γ) and higher sensitivity than has been reported previously. A factorial experiment of developer type, developer temperature, and prebake temperature showed that these are not the main causes of the discrepancy; rather, time between exposure and development appears to account for this difference. Comparison of simulation and SEM micrographs of developed resist profiles gives generally good agreement. An initial study for a much more sensitive resist, ECX-1033, was made and the resist shows promise of solving the thermal effect problem, since it can be exposed at a much lower dose. SAMPLE simulation indicates that the dose required for a similar resist development profile, is only one fifth of that for RD-2000N.

Acknowledgments

I wish to thank Professor Andy Neureuther for his guidance and patience throughout this project. I would also like to thank Dr. R. L. Lozes and P. P. Tang of Perkin-Elmer for the electron-beam exposure with the AEBLE-150 system. Special thanks to G. Addiego for writing the Monte Carlo simulation program for the energy deposition calculation. Thanks also to K. A. Barnett of Hughes Research Laboratory for the characterization of RD-2000N with exposure on System 2. Finally, I would like to thank Kent Cooper of Hughes Research Laboratory for making the SEM photographs of ECX-1033.

This work was supported by Hughes Aircraft Company under the California State MICRO program 86-220 and 87-089.

Table of Contents

Chapter 1

Introduction

Direct-write electron-beam lithography systems have made it desirable to take advantage of the plasma etching resistance of optical resists and to use electron-beam exposure interchangeably in established optical fabrication lines. However, the usual technique of characterizing photoresist by a thickness-remaining versus log-dose curve for each combination of resist thickness, substrate, etc., is time-consuming, and the result does not contain sufficient information for computer simulation of dissolution. The basic objectives of this research are to develop a more fundamental model which can be used in computer simulation and to be able to extract the parameters automatically from experimental measurements.

Perkin-Elmer's development rate monitor (DRM) allows easy measurement of the dissolution rate as a function of depth into the resist layer. These data can then be coupled with Monte Carlo simulations of electron energy deposition in resist. This coupling of dissolution rate with simulated energy states of resist is calculated by SAMPLE[1] using software analogous to that established for optical resist modeling.[2] The result is a model for the dissolution rate of the resist as a function of the energy density deposited by the electron-beam exposure. This rate function can readily be incorporated into the process simulator SAMPLE for development profile simulation.

Two resists of interest in such applications were investigated. The first was the negative type resist, RD-2000N, from the Hitachi Chemical Co., Ltd.[3] Its development characteristics are very similar to the non-swelling dissolution of positive resist, and the dissolution rate appears to be related to the change in molecular weight produced by exposure.[4] Its use with electron-beam exposure has been studied by Okazaki et al.[5] and Liu et al.[6] The second was also a negative type resist, ECX-1033, from the Shipley Co. The chemistry of this resist is based on an acid-hardening resin (AHR) system.[7] The resist is composed of a novolak resin, coupled with an acid-activatable crosslinker and a photoacid generator (PAG). Exposure converts some of the PAG to acid, and this acid catalyzes the formation of many covalent bonds between the novolak and the crosslinker during the post-exposure bake. The "chemical

amplification''-type reaction in the resist provides high sensitivity. Both RD-2000N and ECX-1033 have good dry-etch resistance because of the aromatic novolak polymer[8] which has been used traditionally as the base resin for most optical diazoquinone positive resists.

This report demonstrates the feasibility of using a dissolution rate formula similar to a molecular-weight-based dissolution model for these resists for process optimization. Chapter 2 will give a brief description of the energy deposition versus depth for PMMA and RD-2000N. Chapter 3 describes the experimental conditions, including a factorial experiment to investigate possible sources of differences in the development characteristics of RD-2000N observed in our experiments on the AEBLE-150. Chapter 4 will present the dissolution model and an explanation of process parameter effects. Chapter 5 gives a comparison of SEM and simulation resist profiles.

Chapter 2

Monte Carlo Simulation of Energy Deposition

1. Input to Monte Carlo Simulation

The inputs to the Monte Carlo simulation program are the beam accelerating voltage, the density and the relative atomic composition of the resist. The resist simulated were RD-2000N and PMMA only.† The relative atomic compositions are (73C:9.6O:69H:6N:1S) for RD-2000N and (5C:2O:8H) for PMMA. A density of 1.3, determined experimentally, was used for RD-2000N, and a density of 1.22 [9] was used for PMMA.

2. Simulation Results

The deposited energy density in RD-2000N versus depth for a large uniform area exposure at a dose of 1 $\mu C/cm^2$ is shown in Figure 1. For comparison, the results for PMMA and a theoretical calculation based on Everhart and Hoff's model[10] are also plotted. These data were obtained by Monte Carlo calculation and in fact are the row averages of the exposure matrix used by SAMPLE for simulating electron-beam lithography. The calculation is for 1-μm thick RD-2000N and PMMA at 20 keV for silicon. For a dose of 1 $\mu C/cm^2$, the energy deposited in RD-2000N is 22 J/cm^3 at the surface, increasing monotonically to about 33 J/cm^3 at the depth of 1 μm. These values are slightly higher than those for PMMA. Although the compositions of RD-2000N and PMMA differ substantially, their energy depositions for large area exposures are very similar. Based on these results, the energy deposition for ECX-1033 is assumed to be the same as for RD-2000N, and it is used in subsequent simulation of the resist development profile for ECX-1033.

† Since ECX-1033 is an experimental product, its composition is proprietary.

Chapter 3

Experimental Procedure

1. Objectives

The experiments can be grouped into three classes. The first group was a factorial experiment to explore the sensitivity of RD-2000N to process parameters. The second consisted of experiments to establish a model and observe beam current density effects for RD-2000N. Finally, as the ECX-1033 became available, an experiment was performed to obtain the parameters for the dissolution model. The wafers for the factorial experiment were supplied by Hughes (W1), and those for the model study were prepared at Berkeley (W2).

2. Wafer Preparation and Electron Beam Exposure

The following process conditions were used as the nominal parameters for all the experiments. Four-inch wafers were first primed with HMDS vapor at room temperature for one minute to improve the adhesion of the resist. The wafers were then spin-coated with 1.0-μm resist and baked at 90°C for 30 minutes. Exposure was done on a Perkin-Elmer AEBLE-150 system at 20 keV at Perkin-Elmer in Hayward, CA. The exposure doses ranged from 2.5 to 100 $\mu C/cm^2$. For ECX-1033, after exposure and prior to development, a hot plate bake at 105°C for two minutes was employed. After exposure and a delay of several hours in transit to Berkeley, the wafers were developed in the DRM with the corresponding developers. A beam current density of $25 A/cm^2$ was used in all cases, except where specifically noted.

3. Process Sensitivity

For RD-2000N, the process parameters of bake condition, developer type, and developer temperature were explored in a 2-level factorial experiment. The bake conditions tested were one hour at 110°C and 30 minutes at 90°C. The two developers used were RD-2000N and Microposit MF312. The developer temperatures were set at 18 and 22°C. The second group of experiments involved changes in the state of the developer as well as in beam current density and delay in processing. For ECX-1033,

only an initial dissolution-rate versus deposited-energy curve was generated. The sensitivity of ECX-1033 to a number of process parameters has been thoroughly investigated by Liu, et al.[7]

Chapter 4

Dissolution Model and Experimental Result

1. Dissolution Model

Figure 2 shows a typical dissolution rate of RD-2000N as a function of remaining resist thickness at a dose of 15 $\mu C/cm^2$ at $5A/cm^2$. As expected for a negative resist, the dissolution rate decreases at lower depths because more energy is absorbed. These rate measurements are then combined with the data on deposited energy versus depth from Figure 1. The resulting data on dissolution rate as a function of absorbed energy of RD-2000N is shown in Figure 3. A model similar to that used for the effects of molecular weight on dissolution rate[11,12] was used to fit these data, and the dissolution rate as a function of absorbed energy is given by

$$R = \frac{R_0}{\left(1 + \frac{E}{E_0}\right)^{\alpha}} \tag{1}$$

Here R_0 denotes the development rate of unexposed resist, E_0 is the energy per unit volume at the knee where the asymptote for high dose meets the unexposed rate, and α is the resist-contrast parameter. The parameters for the curve shown are 180 A/sec for R_0, 1360 J/cm^3 for E_0, and 6.72 for α as determined by the computer program PARMEX.[13]

To test its validity, the model was compared with the rate-versus-dose characteristics of RD-2000N for 5 A/cm^2. Figure 4 shows the measurements of thickness remaining as a function of log-dose at various development times. The data calculated by equation (1) with SAMPLE for 120-second development are plotted as diamonds in Figure 4. The calculated thicknesses agrees excellently with the experimental data. Thus our fundamental quantitative resist model correctly describes the experimental data for large uniform exposures and is easily implemented into profile simulation for other resist thicknesses, substrate atomic numbers, and other parameters.

2. Beam Current Density Effects

The effect of dose rate was investigated using 5, 10, and 25 A/cm^2 beam current densities. Fig-

ure 5 shows thickness remaining as a function of log-dose for 90-second development at these beam current densities. The 5-A/cm^2 data shows a slight lateral shift, but this is probably due to dose inaccurate calibration at a very short dwell time. More important is the change in the shape of the curve for 25A/cm^2 above 0.8-μm thickness at high dose. A noticeable flattening of the curve that occurs at 25A/cm^2 corresponds to additional resist top loss. The SEM micrograph in Figure 7c of the resist remaining on the wafer at high beam current density also shows a rough topography. A significant decrease was observed in reflected signal intensity in the DRM measurement as further evidence of the nonplanar topography. These effects were not observed in the 5-A/cm^2 and 10-A/cm^2 cases.

Heating caused by the large beam current on the AEBLE-150 is the likely explanation for the difference in resist performance near the top surface of the resist. With a high beam current density, large exposure area, and fast energy deposition, the temperature of resist exposed by the AEBLE-150 will rise by as much as 100°C. For example, without heat conduction to the substrate, the peak transient temperature rise during exposure would be about 15°C per μC/cm^2. Unless the resist is moderately thermal-conductive, the temperature in the resist will rise with distance from the substrate, and will become substantial even in the presence of a substrate heat sink.

3. Exposure System Effects

We were concerned that the basic behavior of RD-2000N for AEBLE-150 exposure appeared to be different from that reported for other exposure systems. A comparison of the critical dose and contrast is listed in Table I for various exposure and process conditions. Our initial result of a contrast of 0.99 for 25A/cm^2 was quite low compared to those measured for the example on System 2 at Hughes, which showed twice the contrast but required higher doses.

4. Process Parameter Effects

Effects of developer type, developer temperature, and bake temperature on the development of RD-2000N were investigated systematically using the factorial experiment described earlier. The results in Table II reveal that MF312 developer gives higher γ (30-40%) and faster development (40-50%) of unexposed resist (R_0) than the RD-2000N developer. Higher developer temperatures have similar

effects on γ and development rate with MF312 developer (15% increase in γ and 20% increase in R_0). The effect of developer temperature on the RD-2000N development is inconclusive. On the other hand, higher bake temperatures reduce γ (5-8%) and development rate (8-21%). Nonetheless, the γ obtained under the most favorable conditions is still 40% lower than the value measured with exposure from System 2 at Hughes.

5. Sources of Discrepancies

In order to explain the difference in γ and the extrapolated dose for 1.0 normalized thickness-remaining, D(1.0), other possible sources of discrepancies were investigated. The contrast and sensitivity for RD-2000N measured under experimental conditions at Berkeley (row three of Table I) were confirmed by independent experiments at Hughes (AEBLE-150 Hand Dip data, row 4, Table I). Repetition of the experiment four months later with wafers prepared at Berkeley (W2), the same pattern tape (P2), and the same developer (B1) gave slightly higher γ (row 5, Table I). The contrast of the wafer with the same process, but with a fresh bottle of RD-2000N developer (B2) shows an even higher γ (row 6, Table I). Results for resist exposed at 5A/cm^2 with identical conditions gave nearly identical D(1.0) and γ as determined by the DRM, despite the significant difference in top loss at high dose. Since all the above experiments had some delay between exposure and development ranging from 2 days to as much as a week, experiments were performed to investigate this effect. Results for a wafer from the same exposure batch developed after a delay of 20 days (D20) (row 7, Table I) showed significant loss of contrast. Finally, a recent experiment performed at Perkin-Elmer with a delay of less than 1 day (D0) (row 9, Table I) and an aged developer (B3) showed contrast comparable to that of the 5 A/cm^2 experiment. Thus the gradual changes in the resist after exposure may account for the low contrast observed in most of our experiments.

Chapter 5

1. Profile Simulations and SEM Micrograph Comparison

2. Simulation of RD-2000N

Equation (1) has been implemented in the process simulator SAMPLE to study resist development profile effects. A comparison between simulated and experimental resist profiles of RD-2000N is given in Figures 6 and 7. Figure 6 shows the cross-sectional SEM micrograph and simulated resist profiles of a 0.3 μm line for doses of 50, 125, and 250 μC/cm^2 after 120-second development in RD-2000N developer. Figure 7 shows a similar comparison for a constant dose of 63 μC/cm^2 for linewidths of 0.3, 0.5, and 1.0 μm.

3. Simulation of ECX-1033

Using the PARMEX program, the parameters of ECX-1033 were obtained from the DRM dissolution rate measurement. Figure 8 shows the dissolution rate versus absorbed energy and the values predicted by the model. The parameters for the curve shown are 216 A/sec for R_0, 300 J/cm^3 for E_0, and 8.27 for α. This curve shows that ECX-1033 is superior in both sensitivity and contrast to RD-2000N. A comparison between RD-2000N and ECX-1033 was made by adjusting the dose to obtain the same development profile. Figure 9 shows the resulting development profile of a 0.5-μm line for ECX-1033; the dose used is 12 μC/cm^2 for a two-minute development. Comparing Figure 9 to Figure 7b shows that the dose used for ECX-1033 is only one fifth of that for RD-2000N. Figure 10 shows the SEM photographs of the same patterns developed in RD-2000N and ECX-1033. Unlike RD-2000N, ECX-1033 displays no loss in thickness at the flash center of the exposure, evidently, because of the absence of electron-beam induced heating in the ECX-1033.

4. Summary

Generally good agreement is obtained between simulation and experiment, especially considering the large dose range used. The SEM photographs also reveal the nonplanar topography of the resist profiles at large linewidths as shown for example in Figure 7c, which is believed to result from thermal

effects. The discerning eye can, however, spot some fundamental differences between the simulated and experimental profiles that indicate a need to generalize the dissolution model further. The rectangular tops in the simulations result from fitting the dissolution model to 5A/cm^2 data, which did not show a significant top loss at high dose. The larger pedestal at high dose in the simulation may indicate that the algebraic relationship used to model dissolution does not give enough downward curvature with dose to extrapolate well to deposited energy densities over 2 kJ/cm^3.

Chapter 6

Conclusion

Resist dissolution measurement on a Perkin-Elmer Development Rate Monitor and SAMPLE simulation have been used to characterize and model negative resists as exposed on the AEBLE-150 to explore such issues as the effect of different current densities. A quantitative model with three parameters relating dissolution-rate to deposited-energy has been established which fits the thickness versus log dose curve and is suitable for use in process simulation with SAMPLE. For RD-2000N, a high beam current density of $25A/cm^2$ increases the resist thickness top loss at high doses and causes the surface of the resist to become rough, probably through heating. Initially, the resist contrast of RD-2000N (γ) was lower than reported elsewhere. A factorial experiment on process conditions showed that MF312 developer, lower bake temperatures, and higher developer temperatures increase γ and sensitivity, but not strongly enough to account for the observed differences. In hindsight, it appears that the reduced contrast probably results from the delay between exposure and development. Detailed comparison of SEM and simulation profiles gave generally good results over a large range of doses and feature sizes. It also showed that the downward curvature of the model may not be adequate and that it will be necessary to extend the model to include high current density top loss effects. ECX-1033 has higher sensitivity and contrast than RD-2000N because of its "chemical amplification"-type mechanism. Since these characteristics allow a lower beam current density to be used for exposures while maintaining high throughput, it may offer a solution to the problem of thermal effects.

References

1. *SAMPLE User's Guide*, Version 1.6a, University of California, Berkeley, 1985.

2. John Hayes, William R. Bell II, Richard Ferguson, Andrew R. Neureuther, "Resist Characterization on Reflecting Substrates," *SPIE Proceedings*, vol. 631, p. 8, 1986.

3. T. Iwayanagi, T. Kohashi, S. Nonogaki, T. Matsuzawa, H. Douta, and H. Yanazawa, "Azide-Phenolic Resin Photoresists for Deep UV Lithography," *IEEE Transactions on Electron Devices*, vol. ED-28, no. 11, p. 1306, 1981.

4. Michiaki Hashimoto, Takao Iwayanagi, Hiroshi Shiraishi, and Saburo Nonogaki, "Photochemistry of Azide-Phenolic Resin Photoresists," *Polymer Engineering and Science*, vol. 26, no. 16, p. 1090, Mid-September, 1986.

5. S. Okazaki, F. Murai, O. Suga, H. Shiraishi, and S. Koibuchi, *Journal of Vacuum Science and Technology*, vol. B (5), p. 402, 1987.

6. Hua-Yu Liu and E. D. Liu, "Application of GHOST Proximity Effect Correction Method to Conventional and Nonswelling Negative E-beam Resists," *SPIE Proceedings*, vol. 632, p. 244, 1986.

7. Hua-Yu Liu, Mark P. deGrandpre, and Wayne E. Feely, "Characterization of a High Resolution Novolak Based Negative E-beam Resist with 4uC/cm2 Sensitivity," *Journal of Vacuum Science and Technology*, vol. B6 (1), pp. 379-383, Jan/Feb 1988.

8. J. Pacansky, *Journal of Polymer Engineering and Science*, vol. 20, p. 1049, 1980.

9. N. Eib, D. Kyser, and R. Pyle, *VLSI Electronics: Microstructure Science*, 16, p. 111, Academic Press, New York, 1987.

10. T. E. Everhart and P. H. Hoff, *Journal of Applied Physics*, vol. 42, p. 5837, 1971.

11. F. Asmussen and K. Ueberreiter, "Velocity of Dissolution of Polymers. Part II," *Journal of Polymer Science*, vol. 57, p. 199, 1962.

12. G. R. Brewer, ed., J. S. Greeneich, *Electron-Beam in Microelectronic Fabrication*, pp. 98-99, Academic Press, New York, 1980.

13. W.R. Bell II, P.D. Flanner III, C. Zee, N. Tam, and A.R. Neureuther, "Determination of Quantitative Resist Models from Experiment," *SPIE Proceedings*, vol. 920, Santa Clara, Feb. 1988. Advances in Resist Technology and Processing V

Table I. Sensitivity and Contrast of RD-2000N under various process and exposure conditions.

System	Method	Thickness (μm)	Dev. Time (s)	D(1.0) μC/cm^2	γ
Hughes (System 2)	Hand Dip	1.0	90	66	2.4
H.P. (JEOL)	Hand Dip	0.7	100	43	2.0
AEBLE-150	DRM	1.0	120		
25A/cm^2	W1, P2, B1			25	1.0
25A/cm^2	W1, P1, Hand Dip			30	0.99
25A/cm^2	W2, P2, B1			21	1.25
25A/cm^2	W2, P2, B2			29	1.5
25A/cm^2	W2, P2, B2, D20			27	1.25
5A/cm^2	W2, P2, B2	1.0	120	30	1.43
25A/cm^2	W2, P2, B3, D0	1.3	120	29	1.41

W1 - Wafers from Hughes
W2 - Wafers from Berkeley
P1 - Exposure Pattern of Hughes
P2 - Exposure Pattern of Berkeley
B1 - RD-2000N developer batch used in the factorial experiment
B2 - Fresh batch of RD-2000N developer
B3 - RD-2000N developer batch used for more than 15 wafers in 4 months
D0 - Delay of less than 1 day between exposure and development
D20 - Delay of twenty days between exposure and development

Table II. Unexposed resist dissolution rate and contrast of RD-2000N as a funciton of developer type, bake condition, and developer temperature.

Developer	Bake Conditions	Dev. Temp.	R_o (A/sec)	γ
RD2000N	90°C, 30 min	18°C	136	0.99
		22°C	144	0.99
	110°C, 60 min	18°C	107	0.85
		22°C	126	1.09
MF312	90°C, 30 min	18°C	187	1.29
		22°C	217	1.44
	110°C, 60 min	18°C	153	1.18
		22°C	189	1.36

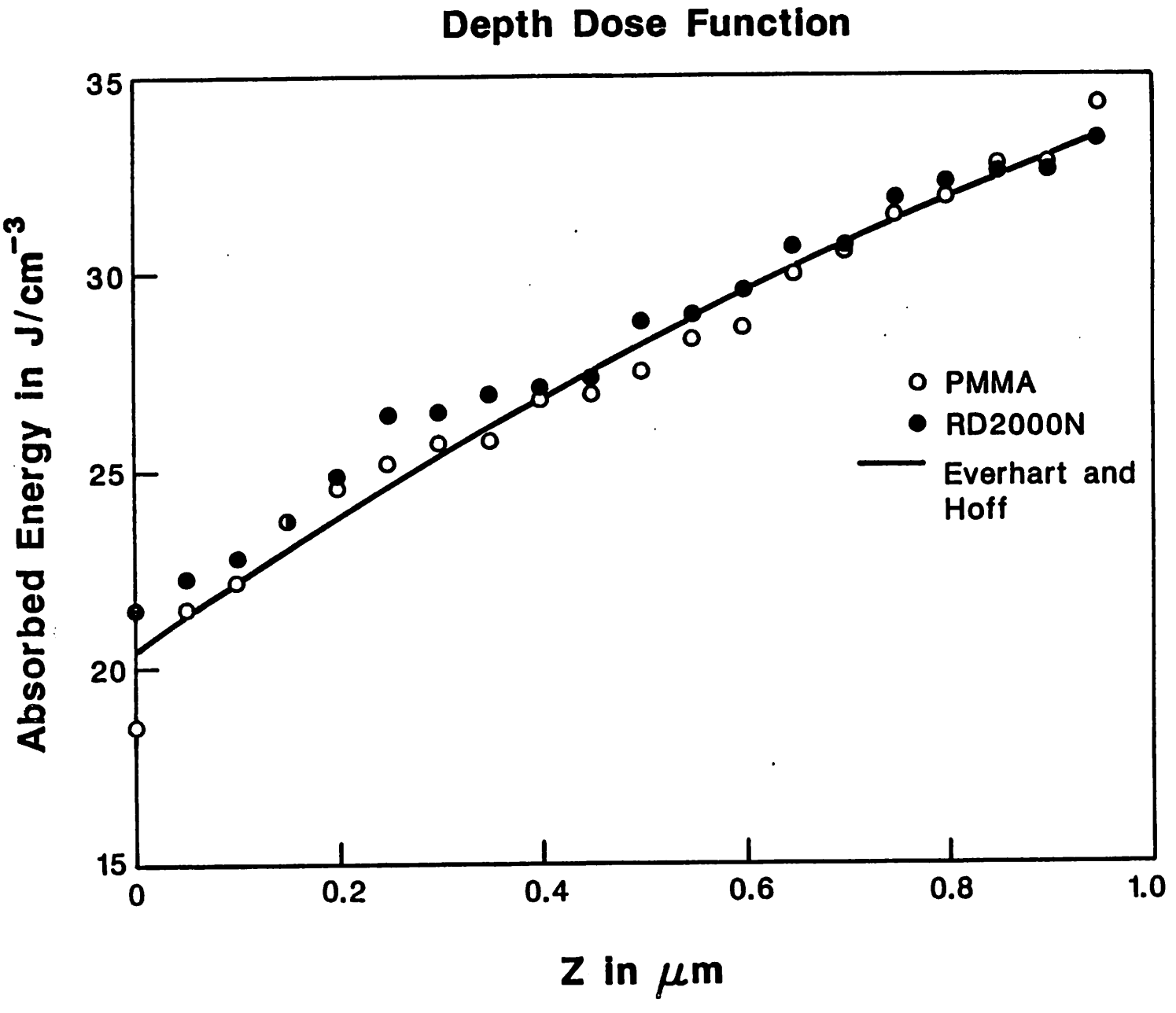

Figure 1. Absorbed energy density for 1 μm RD-2000N and PMMA at 20 keV beam voltage for 1μC/cm^2.

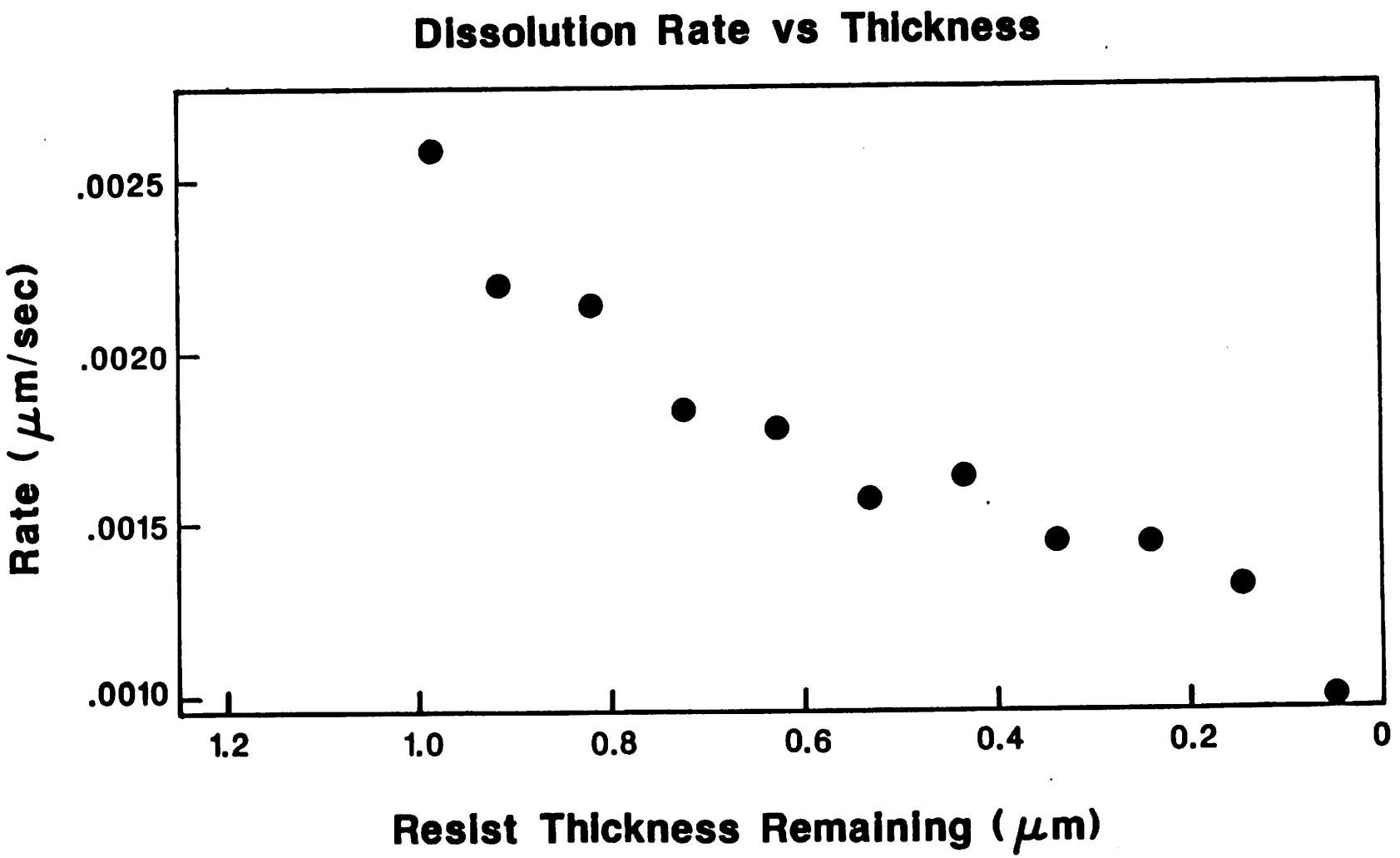

Figure 2. Typical dissolution rate vs depth data for RD-2000N as measured by the DRM at dose of 15μC/cm^2.

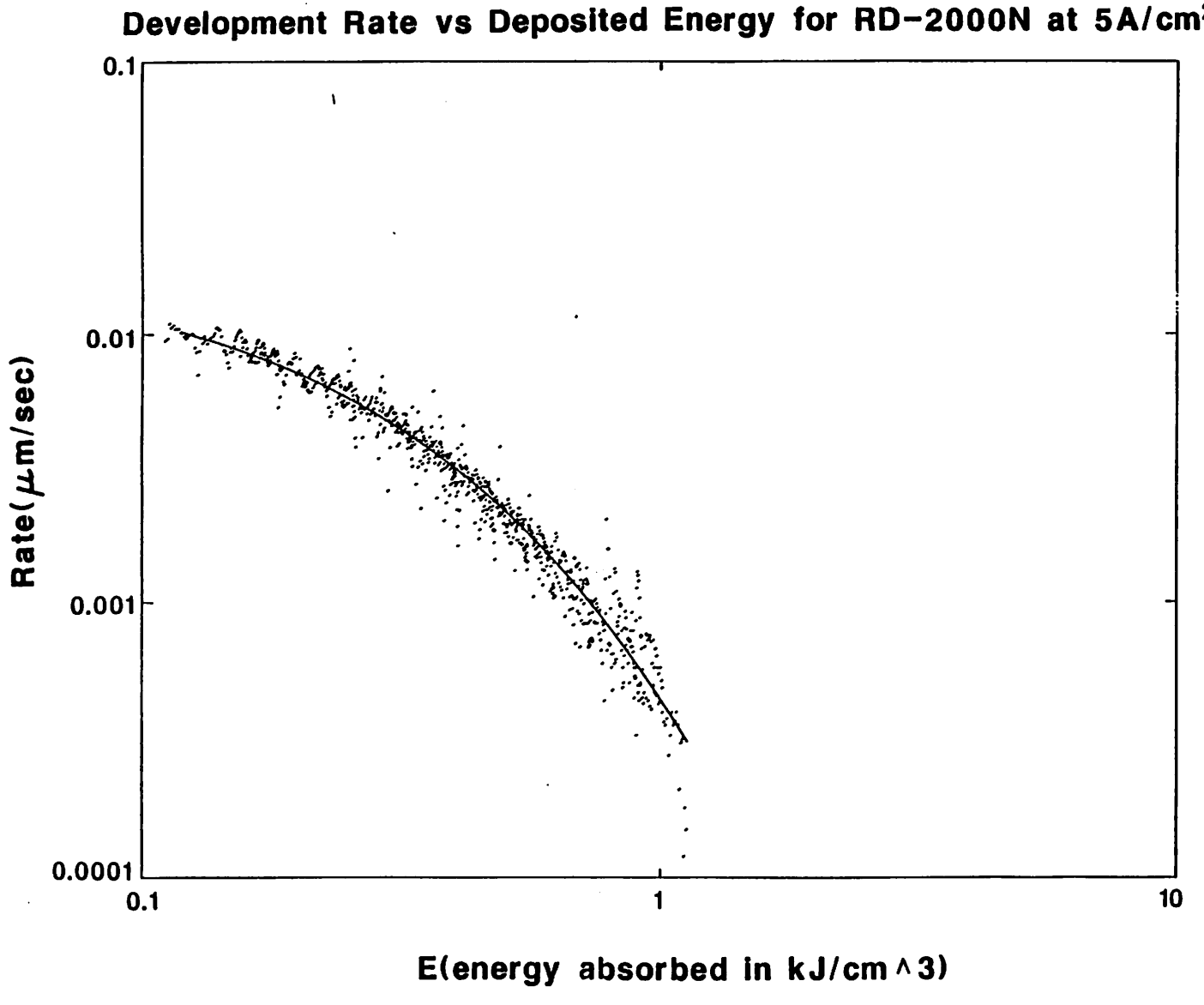

Figure 3. Dissolution rate vs. absorbed energy density for RD-20000N at 5 A/cm^2 beam current density.

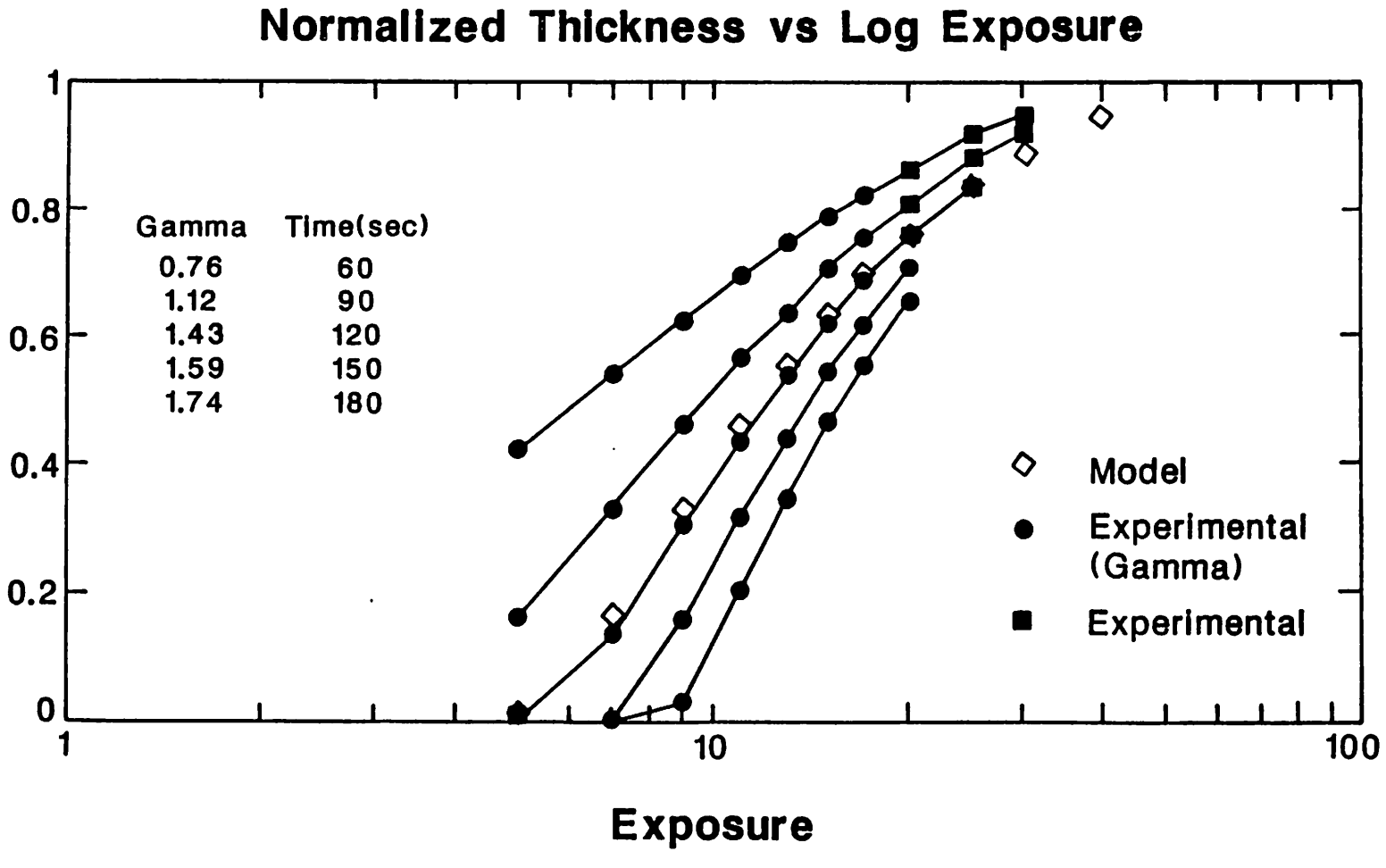

Figure 4. Normalized thickness remaining vs. dose curve for RD-2000N for 60, 90, 120, 150, 180 second development times.

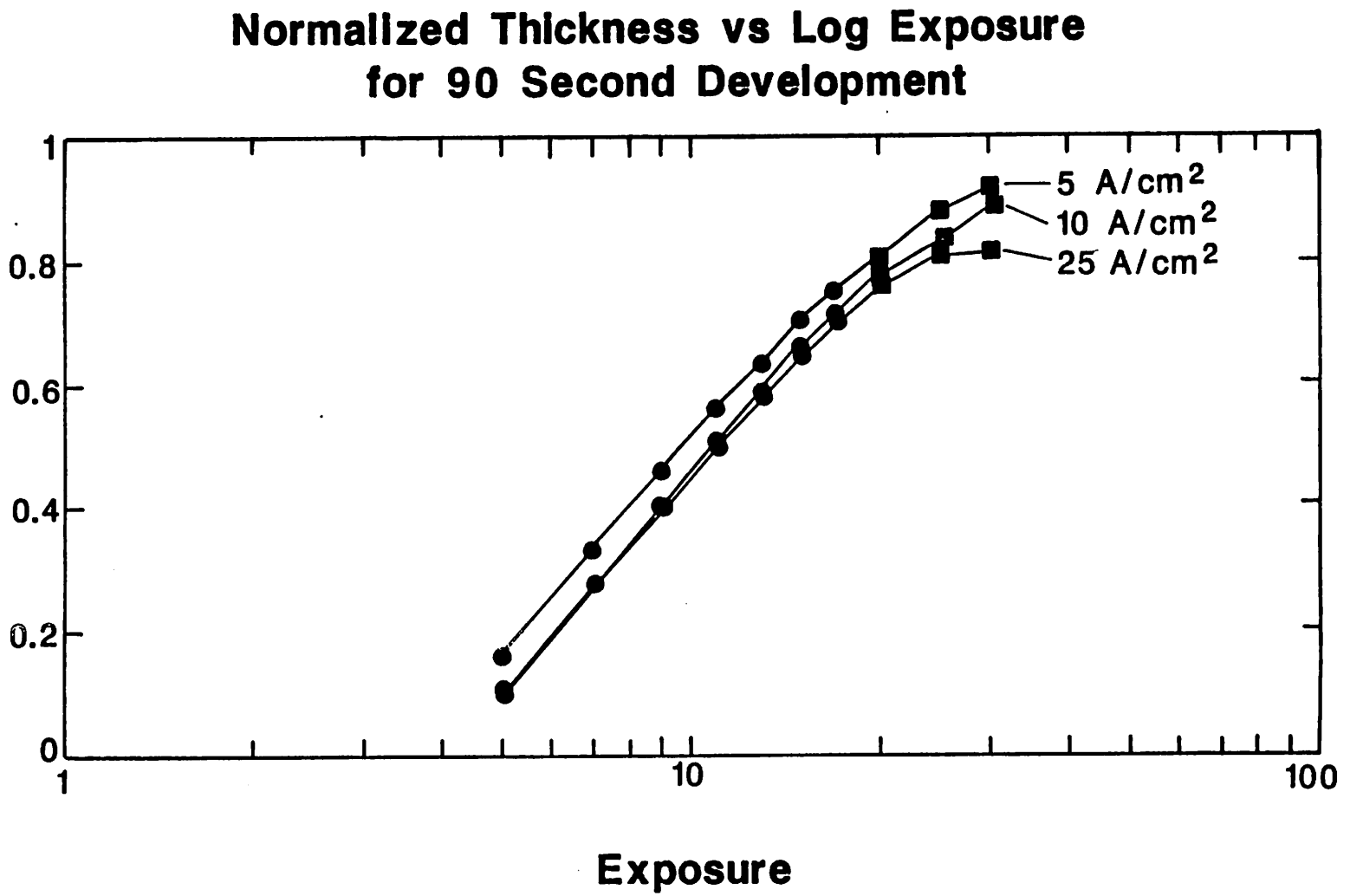

Figure 5. Normalized thickness remaining vs. dose curves for RD-2000N for 90 second development at beam current densities of 5, 10, and 25 A/cm^2.

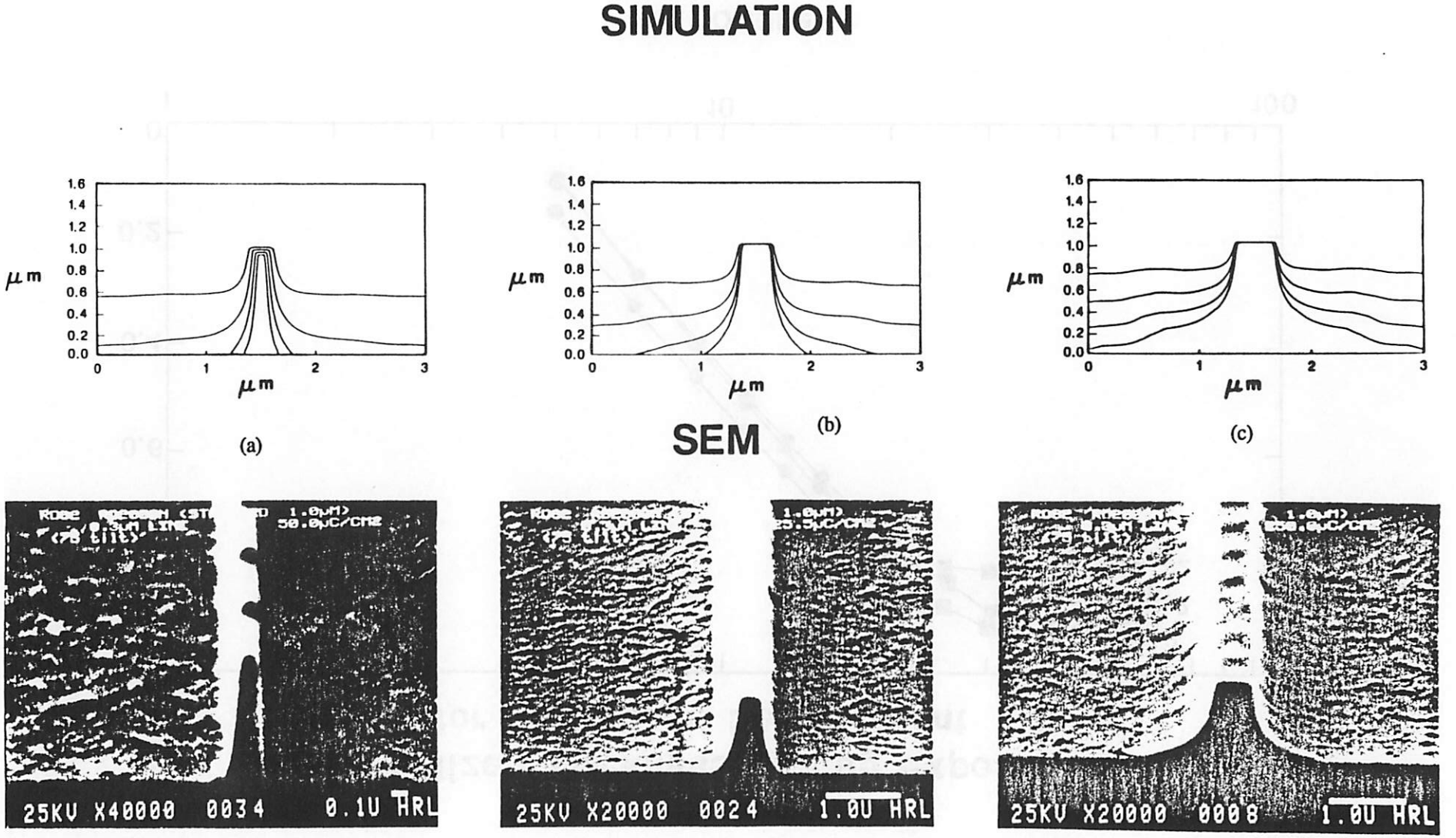

Figure 6. SEM and simulated resist profiles for a 0.3 μm line exposed in 1.0 μm of RD-2000N at doses of (a) 50 μC/cm^2, (b) 125 μC/cm^2, and (c) 250 μC/cm^2 with 2 min development.

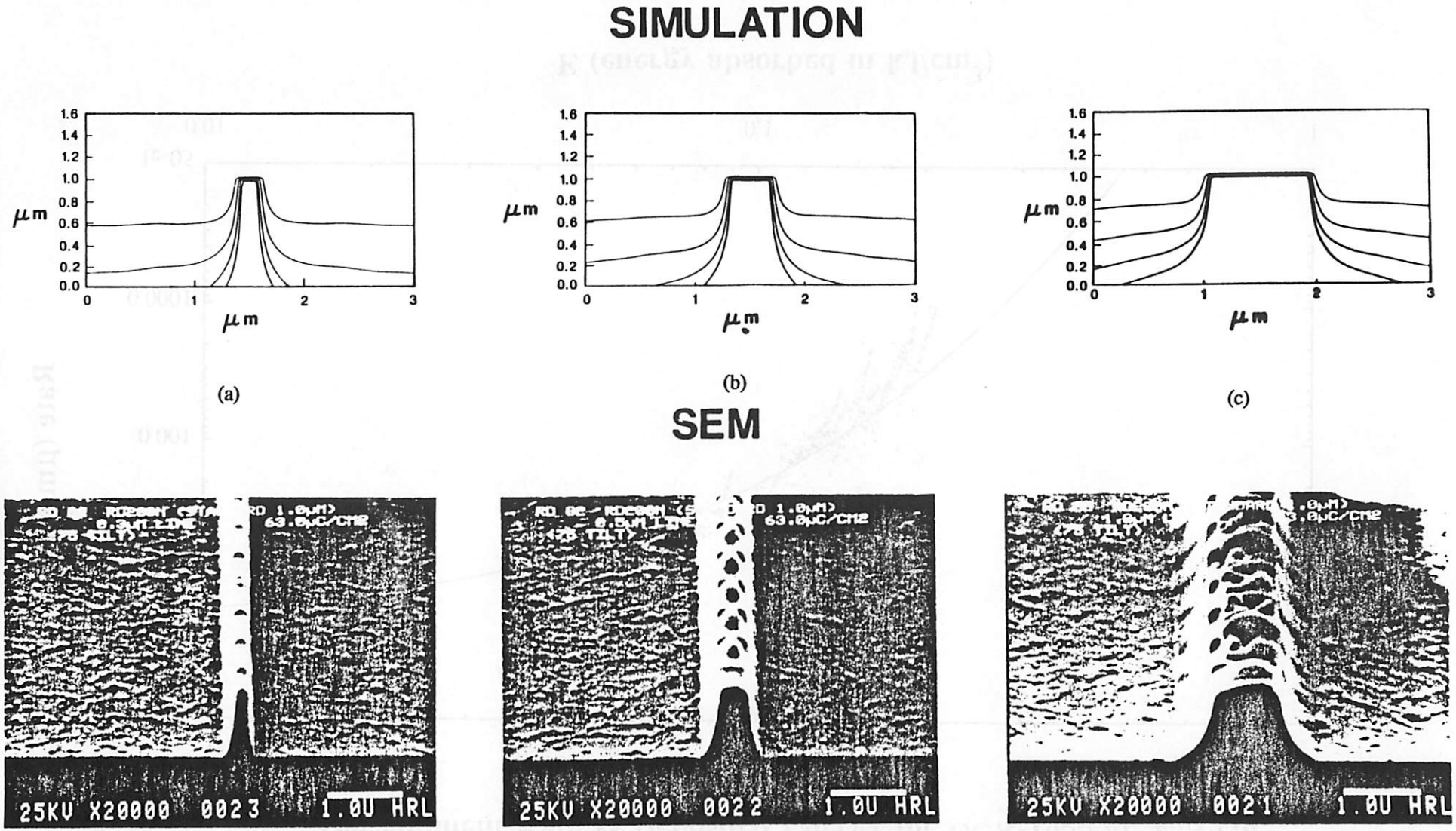

Figure 7. SEM and simulated resist profiles for a single line exposed in 1.0 μm of RD-2000N at dose of 63μC/cm^2 with linewidth of (a) 0.3 μm, 0.5 μm, and 1.0μm with 2 min development.

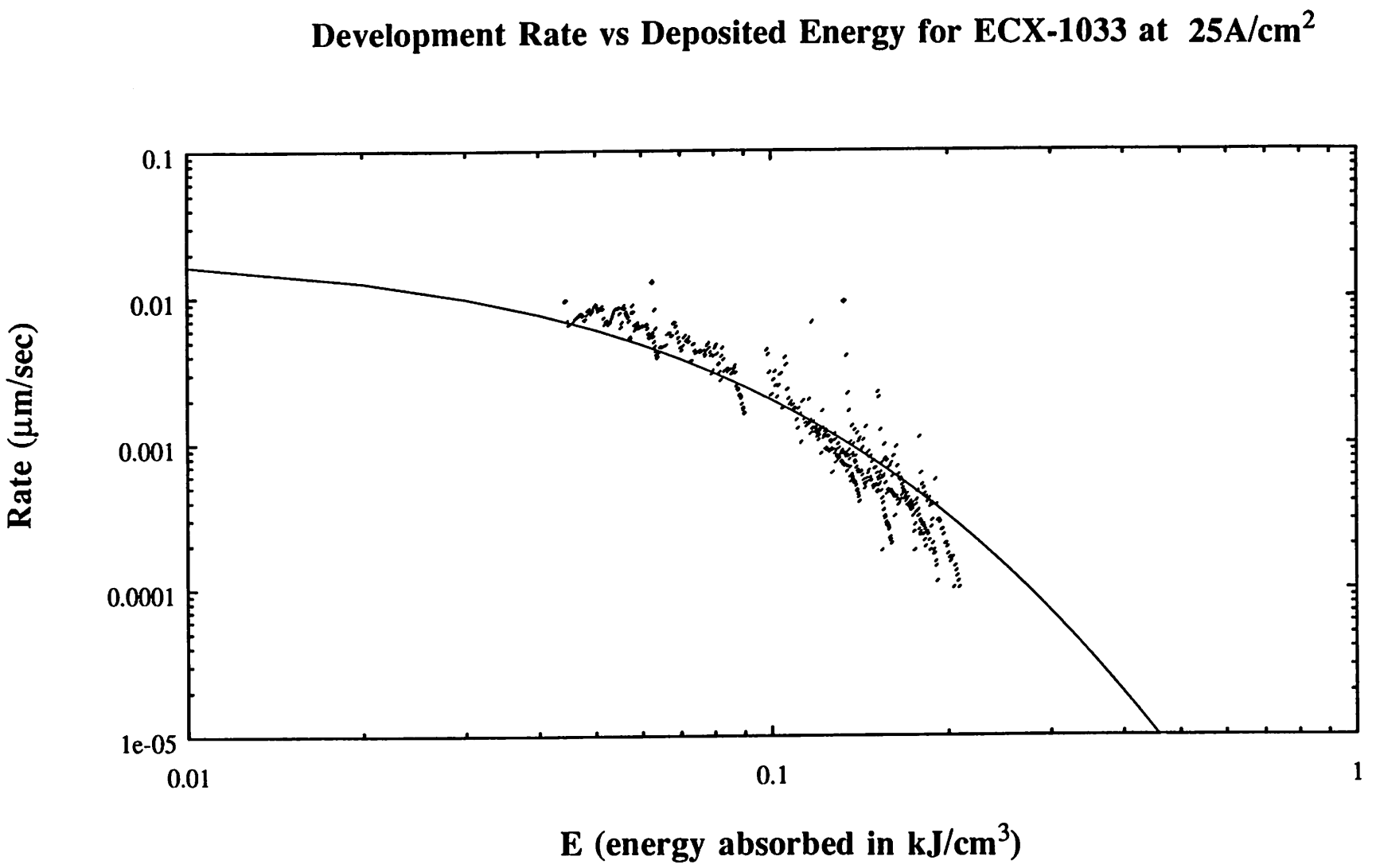

Figure 8. Dissolution rate vs. absorbed energy density for ECX-1033 at 25 A/cm^2 beam current density.

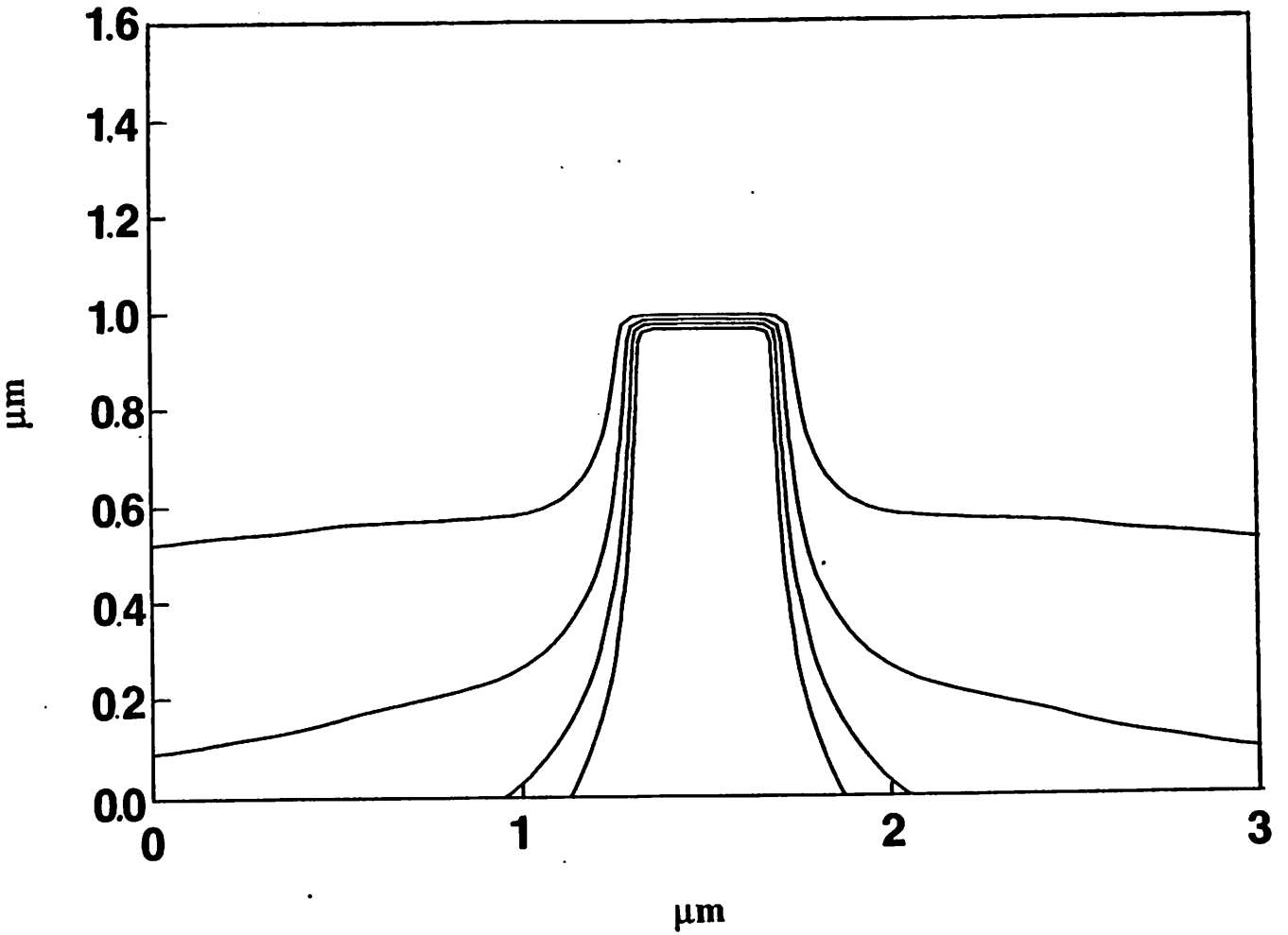

Figure 9. Simulated resist profiles for a 0.5 µm line exposed in 1.0 µm of ECX-1033 at dose of 12 $\mu C/cm^2$ with 2 min development.

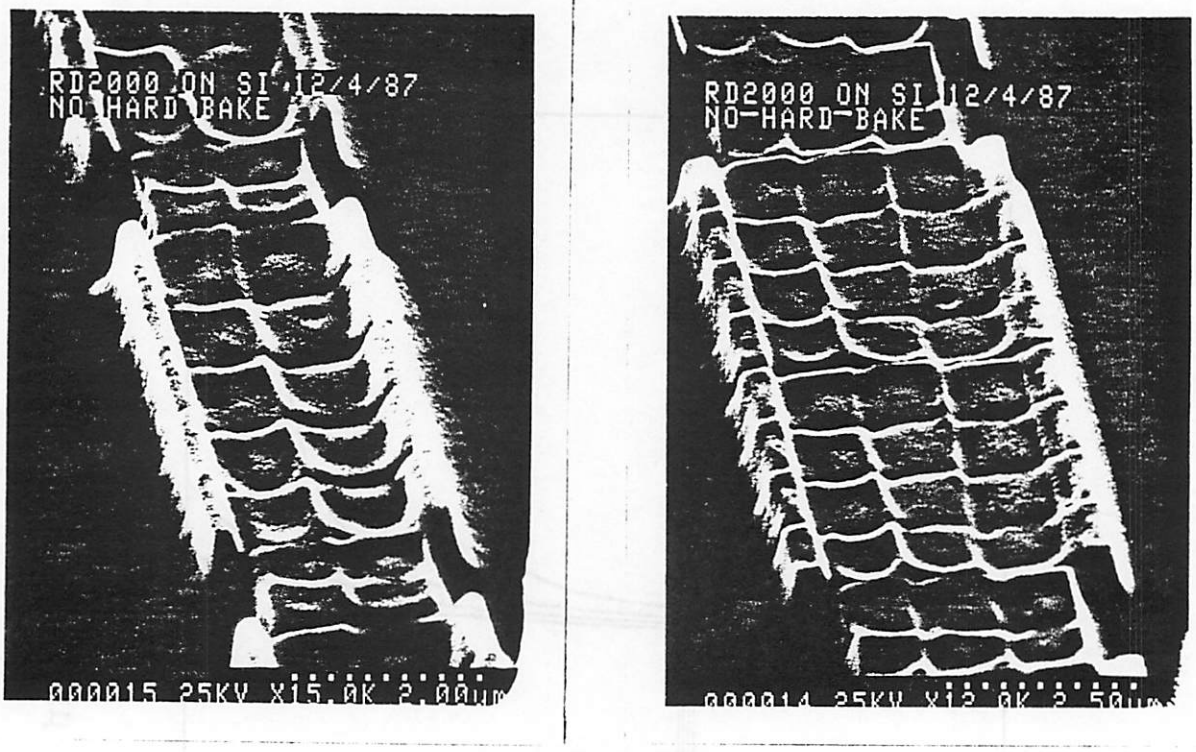

(a)

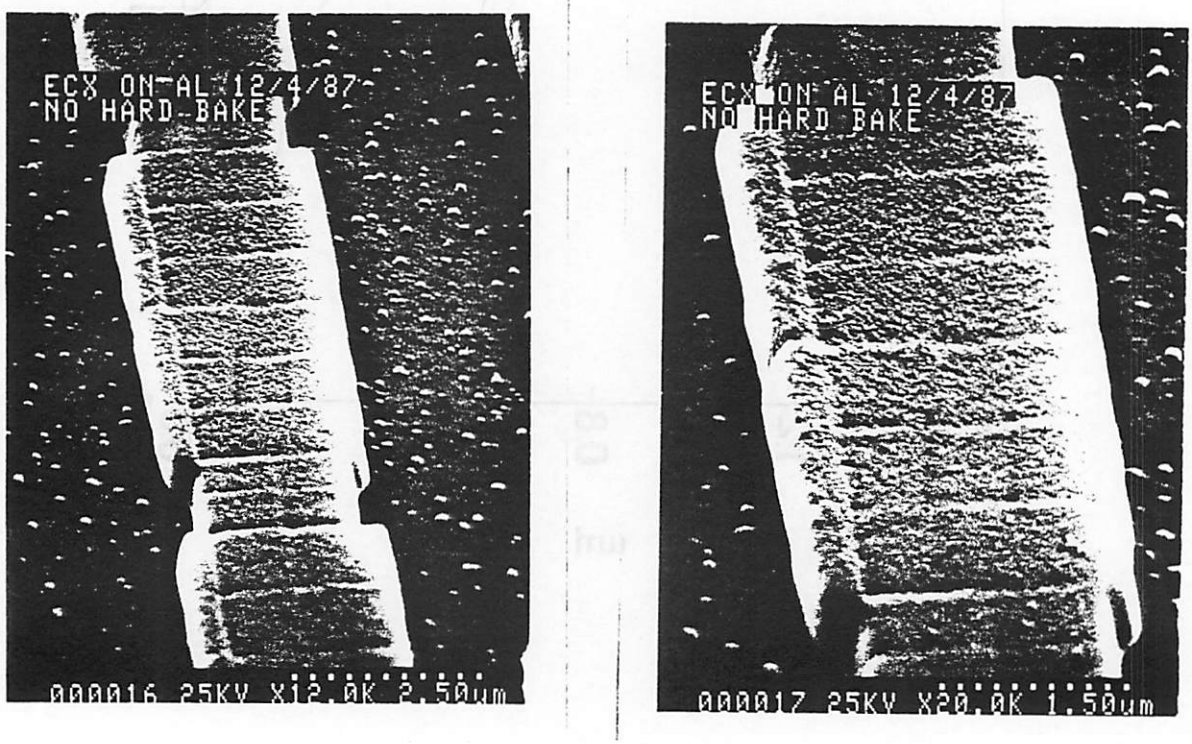

(b)

Figure 10. SEM photographs of developed resist patterns for (a) RD-2000N and (b) ECX-1033. ECX-1033 does not display loss in thickness at flash center as is the case with RD-2000N.